International Journal of Innovative Computing, Information and Control
Volume **12**, Number **3**, June **2016**

ICIC International ©2016 ISSN 1349-4198
pp. 929–940

BACKSTEPPING-BASED TERMINAL SLIDING MODE CONTROL FOR RENDEZVOUS AND DOCKING WITH A TUMBLING SPACECRAFT

Hailong Liu, Xiaoping Shi, Xianting Bi and Jie Zhang

School of Astronautics
Harbin Institute of Technology
No. 92, West Dazhi Street, Nangang District, Harbin 150001, P. R. China
11B904016@hit.edu.cn

Received December 2015; revised March 2016

Abstract. *A chattering free terminal sliding mode controller combining second order nonsingular terminal mode control with backstepping method is proposed for rendezvous and docking with a tumbling target spacecraft, in which disturbances and coupled factors are considered. Firstly, the relative position and relative attitude model are established based on the orbit coordinate system and body coordinate system respectively. Secondly, in order to solve the chattering problem in sliding mode control systems and singularity in terminal sliding mode control systems, this paper proposes a chattering free nonsingular terminal sliding mode control scheme by combining the second order nonsingular terminal mode with backstepping method. The stability of system is proved based on the Lyaponov stability theory. Numerical simulation demonstrates the efficiency of the proposed control method.*

Keywords: Relative motion, Rendezvous and docking, Sliding control, Backstepping control, Integrated control

1. **Introduction.** Many space missions such as rendezvous and docking with other spacecraft require a spacecraft to perform precise position and attitude maneuvers. In particular, with the continuous increase of orbit activities, there is a growing interest in autonomously servicing satellites on orbit to perform tasks such as spacecraft salvage and repair [1], refueling [2], and debris removal [3]. Several space programs have been proposed as technology demonstration of these tasks. JAXA's ETS-7 [4], NASA's DART program, DARPA's Orbital Express Program [5], and SUMO program [6] are some missions that have been completed or are being developed. Since a non-cooperative spacecraft is free-floating and the relative motion information can only be obtained from measurement instruments, high accuracy orbit and attitude control becomes an important research trend and one of the challenges is the coupling problem between the orbit dynamics and attitude dynamics; therefore, the orbit and attitude integrated control problem draws wide attention of researchers.

Various nonlinear control techniques have been investigated in the past to address this problem, such as sliding mode control [7,8], backstepping technique [9,10], and suboptimal technique. Sliding mode (SM) control is a robust nonlinear control technique that has been applied to the spacecraft. However, in the conventional sliding mode control, the convergence of the states can only be achieved in infinite time. The terminal sliding mode (TSM) control [11,12] is able to achieve fast convergence of the states without spending a large control effort by using a nonlinear sliding surface. A nonsingular terminal sliding mode (NTSM) control is proposed [13] to overcome the singularity problem in the TSM by selection of a suitable fractional power in the discontinuous control law. However, one

major disadvantage of the TSM controller is the chattering phenomenon which comprises high frequency oscillations arising because of the discontinuous control signal. The higher order sliding mode (HOSM) control is investigated in recent years, and is applied to robots and aircraft control [14-16].

Recently, most of the research work is about the control for a tumbling target spacecraft. The coupled control inputs have been considered in [17], and based on the feedback linearization, an integrated coupling control algorithm is proposed. The $\theta - D$ nonlinear optimal control technique has been applied in the work of [18,19]. Unfortunately, the robustness of these controllers is not good enough since the parameters of spacecraft are not precisely known in reality. The traditional SM control [20-22] is an effective approach to deal with uncertainties and inaccuracies of nonlinear systems. Compared with linear hyperplane-based sliding modes, NTSM offers some superior properties such as fast, finite time convergence. So based on the NTSM theory, a composite control law which consists of a feedback control based on NTSM method and a feed-forward compensation term based on finite-time disturbance observer is constructed [23,24], and the major merit of the proposed method is that chattering is substantially reduced because the switching gain of the discontinuous control law is only required to be greater than the bound of disturbance estimation error rather than the disturbance. However, the chattering phenomenon in these studies cannot be totally eliminated and the control signal is still discontinuous.

The HOSM control is an effective method for overcoming the chattering phenomenon that exists in the traditional sliding mode [14-16]. Inspired by this observation, this paper proposes a chattering free nonsingular terminal sliding mode control scheme by combining second order nonsingular terminal mode with backstepping method in order to solve the chattering problem in sliding mode control systems and singularity in terminal sliding mode control systems.

Rest of the paper is organized as follows. Section 2 describes the dynamics of six degree-of-freedom rigid body spacecraft motion. In Section 3, the chattering free terminal sliding mode controller combining second order nonsingular terminal mode control with backstepping method is proposed. Simulation results are presented in Section 4. Conclusions are given in Section 5.

2. Problem Statement and Preliminaries.

In this paper, the tumbling non-cooperative target is supposed to be on the Kepler orbit, so it is possible for the chaser spacecraft to obtain the orbit parameters of the target. Furthermore, it is more reasonable to attach the coordinate system to the mass center of target spacecraft, which is used to describe the relative motion. In this section, the coordinate system used in this paper is defined. Besides, the relative orbit dynamics and the relative attitude dynamics are obtained. Then, the integrated model of relative orbit and relative attitude is established, which is used for the control law design in the following sections.

2.1. Coordinate system.

Figure 1 shows the definition of the coordinate system that is used in this paper. Here, ω_c, ω_t stand for the angular velocity of the chaser and the target spacecraft respectively. The coordinate system $OXYZ$ stands for the earth inertia coordinate system. In order to describe the relative position and relative attitude between the chaser spacecraft and the target spacecraft, the orbit coordinate system is established in the target spacecraft. The mass center of the target spacecraft is defined as the origin of the coordinate system, the x axis is the direction of the target spacecraft velocity, the z axis is along the opposite direction of the earth radius, and the y axis can be fixed by the right hand law.

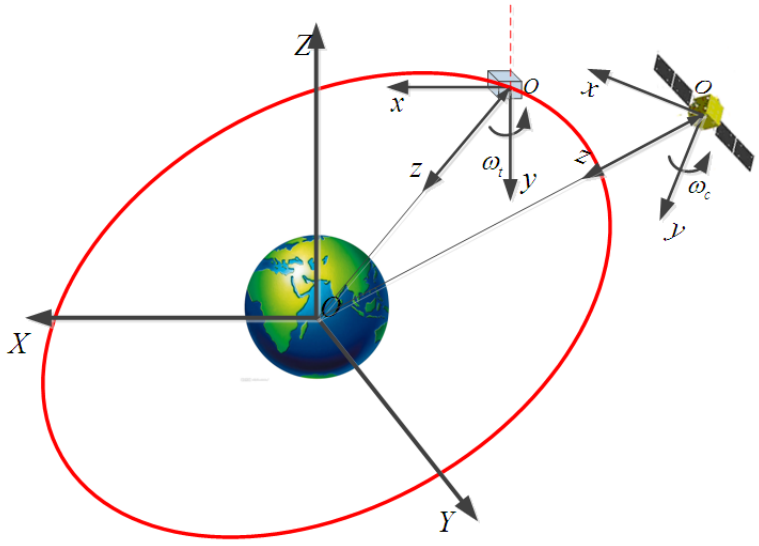

FIGURE 1. Coordinate system definition

2.2. **Relative orbit dynamics.**

Assumption 1 The orbit parameters of the target spacecraft can be known in advance. Based on the above assumption, the following relative orbit dynamics equation seems more reasonable, which includes some orbit parameters of target spacecraft in its equation description. The relative orbit dynamics equation [25] is shown in Equation (1)

$$\begin{cases} \ddot{x} = n^2 x + \dot{n} z + 2n\dot{z} - \dfrac{\mu}{r_c^3} x + f_{dx}/m_c + F_{cx}/m_c \\ \ddot{y} = -\dfrac{\mu}{r_c^3} y + f_{dy}/m_c + F_{cy}/m_c \\ \ddot{z} = -\dot{n} x + n^2 z - 2n\dot{x} - \dfrac{\mu}{r_t^2} - \dfrac{\mu}{r_c^3}(z - r_t) + f_{dz}/m_c + F_{cz}/m_c \end{cases} \tag{1}$$

where x, y, z stand for the relative position vector component between the chaser spacecraft and the target spacecraft; r_c, r_t stand for the orbit radius of the chaser and the target spacecraft respectively; n and $\dot{n}$ stand for the orbit angular velocity and angular acceleration velocity; F_{cx}, F_{cy}, F_{cz} are the control force vector component; f_{dx}, f_{dy}, f_{dz} are the disturbance force vector component; μ is the earth gravitation constant; m_c stands for the mass of the chaser.

The nonlinear relative orbit dynamics mentioned above could be written as Equation (2).

$$\ddot{\boldsymbol{\rho}} = \boldsymbol{M}_1 \boldsymbol{\rho} + \boldsymbol{M}_2 \dot{\boldsymbol{\rho}} + \boldsymbol{M}_3 + \boldsymbol{F}_c/m_c + \boldsymbol{f}_d/m_c \tag{2}$$

where

$$\boldsymbol{\rho} = \begin{bmatrix} x & y & z \end{bmatrix}^{\mathrm{T}}, \quad \boldsymbol{F}_c = \begin{bmatrix} F_{cx} & F_{cy} & F_{cz} \end{bmatrix}^{\mathrm{T}}, \quad \boldsymbol{f}_d = \begin{bmatrix} f_{dx} & f_{dy} & f_{dz} \end{bmatrix}^{\mathrm{T}}$$

$$\boldsymbol{M}_1 = \begin{bmatrix} \dot{\theta}^2 & 0 & \ddot{\theta} \\ 0 & 0 & 0 \\ -\ddot{\theta} & 0 & \dot{\theta}^2 \end{bmatrix}, \quad \boldsymbol{M}_2 = \begin{bmatrix} 0 & 2\dot{\theta} & 0 \\ -2\dot{\theta} & 0 & 0 \\ 0 & 0 & 0 \end{bmatrix}, \quad \boldsymbol{M}_3 = \begin{bmatrix} -\mu x/r_c^3 \\ -\mu y/r_c^3 \\ -\mu/r_t^2 - \mu(z - r_t)/r_c^3 \end{bmatrix}$$

2.3. **Relative attitude dynamics.** In this paper, both the chaser spacecraft and the target spacecraft are considered as the rigid body, and the desired attitude of the chaser spacecraft is the attitude of the target spacecraft. In this subsection, based on the law of the rigid body moment of momentum, the dynamics and kinematics for both the chaser

spacecraft and target spacecraft are established, and then the relative attitude dynamics is obtained.

Firstly, based on the rigid body moment of momentum, the attitude dynamics of the chaser spacecraft can be obtained as Equation (3)

$$\boldsymbol{I}_c\dot{\boldsymbol{\omega}}_c + \tilde{\boldsymbol{\omega}}_c\boldsymbol{I}_c\boldsymbol{\omega}_c = \boldsymbol{\tau}_c + \boldsymbol{\tau}_{dc} \tag{3}$$

where $\boldsymbol{I}_c$ is the moment of inertia of the chaser spacecraft, $\boldsymbol{\omega}_c$ is its angular velocity, $\boldsymbol{\tau}_c$, $\boldsymbol{\tau}_{dc}$ are the control torque and disturbance torque respectively. Furthermore, this paper defines skew symmetric matrix for arbitrary vector $\boldsymbol{a} = \begin{bmatrix} a_x & a_y & a_z \end{bmatrix}^{\mathrm{T}}$ as Equation (4)

$$\tilde{\boldsymbol{a}} = \begin{bmatrix} 0 & -a_z & a_y \\ a_z & 0 & -a_x \\ -a_y & a_x & 0 \end{bmatrix} \tag{4}$$

And the kinematics of the chaser spacecraft could be described as the following equation

$$\dot{\boldsymbol{q}}_c = \frac{1}{2}\begin{bmatrix} 0 & -\boldsymbol{\omega}_c^{\mathrm{T}} \\ \boldsymbol{\omega}_c & -\tilde{\boldsymbol{\omega}}_c \end{bmatrix}\boldsymbol{q}_c \tag{5}$$

where $\boldsymbol{q}_c$ is the attitude quaternion of the chaser spacecraft. For arbitrary attitude quaternion $\boldsymbol{q}$, we define $\boldsymbol{q} = \begin{bmatrix} q_0 & \hat{\boldsymbol{q}} \end{bmatrix}^{\mathrm{T}}$. q_0, $\hat{\boldsymbol{q}}$ are the scalar part and the vector part of the quaternion $\boldsymbol{q}$, and they satisfy the following constraint condition

$$q_0^2 + \hat{\boldsymbol{q}}^2 = 1 \tag{6}$$

In a similar way, the dynamics and kinematics equations of the target spacecraft are obtained as Equation (7) and Equation (8)

$$\boldsymbol{I}_t\dot{\boldsymbol{\omega}}_t + \tilde{\boldsymbol{\omega}}_t\boldsymbol{I}_t\boldsymbol{\omega}_t = 0 \tag{7}$$

$$\dot{\boldsymbol{q}}_t = \frac{1}{2}\begin{bmatrix} 0 & -\boldsymbol{\omega}_t^{\mathrm{T}} \\ \boldsymbol{\omega}_t & -\tilde{\boldsymbol{\omega}}_t \end{bmatrix}\boldsymbol{q}_t \tag{8}$$

where $\boldsymbol{I}_t$ is the moment of inertia of the target spacecraft, $\boldsymbol{\omega}_t$ is its angular velocity. $\boldsymbol{q}_t$ is the attitude quaternion of the target spacecraft.

We define $\boldsymbol{q}_r$ as the attitude error quaternion, which can be obtained as Equation (9)

$$\boldsymbol{q}_r = \begin{bmatrix} q_{t0} & \hat{\boldsymbol{q}}_t^{\mathrm{T}} \\ -\hat{\boldsymbol{q}}_t & q_{t0}\boldsymbol{I}_{3\times 3} - \tilde{\hat{\boldsymbol{q}}}_t \end{bmatrix}\boldsymbol{q}_c \tag{9}$$

Furthermore, the attitude error quaternion satisfies the following kinematics equation

$$\dot{\boldsymbol{q}}_r = \frac{1}{2}\begin{bmatrix} 0 & -\boldsymbol{\omega}_r^{\mathrm{T}} \\ \boldsymbol{\omega}_r & -\tilde{\boldsymbol{\omega}}_r \end{bmatrix}\boldsymbol{q}_r \tag{10}$$

where $\boldsymbol{\omega}_r$ is the relative attitude angular velocity, and $\boldsymbol{\omega}_r$ satisfies the following equation

$$\boldsymbol{\omega}_r = \boldsymbol{\omega}_c - \boldsymbol{A}_{ct}\boldsymbol{\omega}_t \tag{11}$$

In Equation (11), $\boldsymbol{A}_{ct}$ is the transform matrix from target spacecraft body coordinate system to the chaser body coordinate system, and $\boldsymbol{A}_{ct}$ could be described by the following equation

$$\boldsymbol{A}_{ct} = \boldsymbol{A}(\boldsymbol{q}_e) = \left(q_{e0}^2 - \hat{\boldsymbol{q}}_e^{\mathrm{T}}\hat{\boldsymbol{q}}_e\right)\boldsymbol{I}_{3\times 3} + 2\hat{\boldsymbol{q}}_e^{\mathrm{T}}\hat{\boldsymbol{q}}_e - 2q_{e0}\tilde{\hat{\boldsymbol{q}}}_e \tag{12}$$

Then we can obtain the time derivative of $\boldsymbol{\omega}_r$ as Equation (13)

$$\begin{aligned} \dot{\boldsymbol{\omega}}_r &= \dot{\boldsymbol{\omega}}_c - \boldsymbol{A}_{ct}\dot{\boldsymbol{\omega}}_t + \tilde{\boldsymbol{\omega}}_r\boldsymbol{\omega}_c \\ &= \boldsymbol{I}_c^{-1}\left(\boldsymbol{\tau}_c + \boldsymbol{\tau}_{gc} + \boldsymbol{\tau}_{dc} - \tilde{\boldsymbol{\omega}}_c\boldsymbol{I}_c\boldsymbol{\omega}_c\right) - \boldsymbol{A}_{ct}\dot{\boldsymbol{\omega}}_t + \tilde{\boldsymbol{\omega}}_r\boldsymbol{\omega}_c \\ &= \boldsymbol{t}_c + \boldsymbol{I}_c^{-1}(\boldsymbol{\tau}_c + \boldsymbol{\tau}_{dc}) \end{aligned} \tag{13}$$

where $\boldsymbol{t}_c = -\boldsymbol{I}_c^{-1}\tilde{\boldsymbol{\omega}}_c\boldsymbol{I}_c\boldsymbol{\omega}_c - \boldsymbol{A}_{ct}\dot{\boldsymbol{\omega}}_t + \tilde{\boldsymbol{\omega}}_r\boldsymbol{\omega}_c$.

The time derivative of Equation (10) is given by

$$\begin{aligned}\ddot{\boldsymbol{q}}_r &= \frac{1}{2}\begin{bmatrix} 0 & -\dot{\boldsymbol{\omega}}_r^{\mathrm{T}} \\ \dot{\boldsymbol{\omega}}_r & -\dot{\tilde{\boldsymbol{\omega}}}_r \end{bmatrix}\boldsymbol{q}_r + \frac{1}{2}\begin{bmatrix} 0 & -\boldsymbol{\omega}_r^{\mathrm{T}} \\ \boldsymbol{\omega}_r & -\tilde{\boldsymbol{\omega}}_r \end{bmatrix}\dot{\boldsymbol{q}}_r \\ &= \frac{1}{2}\begin{bmatrix} 0 & -\boldsymbol{t}_c^{\mathrm{T}} \\ \boldsymbol{t}_c & -\tilde{\boldsymbol{t}}_c \end{bmatrix}\boldsymbol{q}_r + \frac{1}{2}\begin{bmatrix} 0 & -\boldsymbol{\omega}_r^{\mathrm{T}} \\ \boldsymbol{\omega}_r & -\tilde{\boldsymbol{\omega}}_r \end{bmatrix}\dot{\boldsymbol{q}}_r + \frac{1}{2}\begin{bmatrix} -\hat{\boldsymbol{q}}_r^{\mathrm{T}} \\ q_{r0}\boldsymbol{I}_{3\times 3} + \tilde{\hat{\boldsymbol{q}}}_r \end{bmatrix}\boldsymbol{I}_c^{-1}\boldsymbol{\tau}_c \end{aligned} \tag{14}$$

The compact form for Equation (14) can be written as the following equation

$$\ddot{\boldsymbol{q}}_r = \frac{1}{2}\boldsymbol{N}_1\boldsymbol{q}_r + \frac{1}{2}\boldsymbol{N}_2\dot{\boldsymbol{q}}_r + \frac{1}{2}\boldsymbol{N}_3\boldsymbol{I}_c^{-1}\boldsymbol{\tau}_c \tag{15}$$

where $\boldsymbol{N}_1 = \begin{bmatrix} 0 & -\boldsymbol{t}_c^{\mathrm{T}} \\ \boldsymbol{t}_c & -\tilde{\boldsymbol{t}}_c \end{bmatrix}$, $\boldsymbol{N}_2 = \begin{bmatrix} 0 & -\boldsymbol{\omega}_r^{\mathrm{T}} \\ \boldsymbol{\omega}_r & -\tilde{\boldsymbol{\omega}}_r \end{bmatrix}$, $\boldsymbol{N}_3 = \begin{bmatrix} -\hat{\boldsymbol{q}}_r^{\mathrm{T}} \\ q_{r0}\boldsymbol{I}_{3\times 3} + \tilde{\hat{\boldsymbol{q}}}_r \end{bmatrix}$.

2.4. **The orbit and attitude integrated dynamics.** Define the system states $\boldsymbol{x}_1 = \begin{bmatrix} \boldsymbol{\rho} & \boldsymbol{q}_r \end{bmatrix}^{\mathrm{T}}$, $\boldsymbol{x}_2 = \begin{bmatrix} \dot{\boldsymbol{\rho}} & \dot{\boldsymbol{q}}_r \end{bmatrix}^{\mathrm{T}}$. Based on the relative orbit dynamics model shown in Equation (2) and the relative attitude dynamics shown in Equation (14), we can obtain the orbit and attitude integrated dynamics as the following equation

$$\begin{cases} \dot{\boldsymbol{x}}_1 = \boldsymbol{x}_2 \\ \dot{\boldsymbol{x}}_2 = \boldsymbol{f} + \boldsymbol{B}\boldsymbol{u} + \boldsymbol{d} \end{cases} \tag{16}$$

where $\boldsymbol{f} = \begin{bmatrix} \boldsymbol{M}_1\boldsymbol{\rho} + \boldsymbol{M}_2\dot{\boldsymbol{\rho}} + \boldsymbol{M}_3(\boldsymbol{\rho}) \\ \frac{1}{2}\boldsymbol{N}_1\boldsymbol{q}_r + \frac{1}{2}\boldsymbol{N}_2\dot{\boldsymbol{q}}_r \end{bmatrix}$, $\boldsymbol{u} = \begin{bmatrix} \boldsymbol{F}_c \\ \boldsymbol{\tau}_c \end{bmatrix}$, $\boldsymbol{B} = \begin{bmatrix} \frac{1}{m_c}\boldsymbol{I}_{3\times 3} & \boldsymbol{0}_{3\times 3} \\ \boldsymbol{0}_{4\times 3} & \frac{1}{2}\boldsymbol{N}_3\boldsymbol{I}_c^{-1} \end{bmatrix}$, $\boldsymbol{d} = \begin{bmatrix} \boldsymbol{f}_d/m_c \\ \frac{1}{2}\boldsymbol{N}_3\boldsymbol{I}_c^{-1}\boldsymbol{\tau}_{dc} \end{bmatrix}$.

3. **Control Design.** NTSM control is a new method developed in recent years, which inherits the advantage of TSM control such as strong robustness and rapid convergence. Besides, NTSM control overcomes the singularity that may occur in the TSM. However, the chattering phenomenon still exists in the control output.

In order to overcome the chattering problem, this paper proposes a new controller by combining second order nonsingular terminal mode control with backstepping method. Using this design method proposed in this paper, a new control law that is chattering free and strong robustness is obtained. In this section, the detailed design steps are introduced.

Step 1 Virtual control design

In this step, the first subsystem closed-loop system (16) is considered:

$$\dot{\boldsymbol{x}}_1 = \boldsymbol{x}_2 \tag{17}$$

The tracking error vectors are defined as the following equations

$$\boldsymbol{z}_1 = \boldsymbol{x}_1 - \boldsymbol{x}_{1d} \tag{18}$$

$$\boldsymbol{z}_2 = \boldsymbol{x}_2 - \boldsymbol{x}_{2d} \tag{19}$$

where $\boldsymbol{x}_{1d}$, $\boldsymbol{x}_{2d}$ are the reference inputs.

Considering Equation (17), the time derivative of Equation (18) is given by

$$\dot{\boldsymbol{z}}_1 = \boldsymbol{x}_2 - \dot{\boldsymbol{x}}_{1d} \tag{20}$$

Based on the result of Equation (20), the virtual control function is designed as Equation (21)

$$\boldsymbol{x}_{2d} = -\boldsymbol{c}_1\boldsymbol{z}_1 + \dot{\boldsymbol{x}}_{1d} \tag{21}$$

where $\boldsymbol{c}_1$ is the feedback gain matrix that is to be designed and $\boldsymbol{c}_1 > 0$.

In order to analyze the stability of subsystem (17), we construct a Lyaponuv function as follows

$$V_1 = \frac{1}{2}\boldsymbol{z}_1^{\mathrm{T}}\boldsymbol{z}_1 \tag{22}$$

Supposing that the second subsystem of system (16) could achieve accurate tracking, that means $\boldsymbol{z}_2 = 0$, then we could obtain the following equation

$$\boldsymbol{x}_2 = \boldsymbol{x}_{2d} = -\boldsymbol{c}_1\boldsymbol{z}_1 + \dot{\boldsymbol{x}}_{1d} \tag{23}$$

The time derivative of V_1 can be obtained as Equation (24)

$$\dot{V}_1 = \boldsymbol{z}_1^{\mathrm{T}}\dot{\boldsymbol{z}}_1 = -\boldsymbol{z}_1^{\mathrm{T}}\boldsymbol{c}_1\boldsymbol{z}_1 \leq 0 \tag{24}$$

Based on the Lyapunov stability theory, the subsystem (18) is asymptotically stable.

Step 2 Designing control law $\boldsymbol{u}$ that makes the tracking error $\boldsymbol{z}_2$ converge to zero in finite time

The second subsystem of closed-loop system (16) is considered

$$\dot{\boldsymbol{x}}_2 = \boldsymbol{f} + \boldsymbol{B}\boldsymbol{u} + \boldsymbol{d} \tag{25}$$

Based on Equation (19) and Equation (16), the tracking error dynamics could be obtained as Equation (26)

$$\dot{\boldsymbol{z}}_2 = \boldsymbol{f} + \boldsymbol{B}\boldsymbol{u} + \boldsymbol{d} - \dot{\boldsymbol{x}}_{2d} \tag{26}$$

If the SM control method is applying here, then only the asymptotic stability can be guaranteed for the tracking error. Based on the second order nonsingular sliding mode control method in this paper, the tracking error $\boldsymbol{z}_2$ converges to zero in finite time. Besides, this method proposed in this paper can void the singular phenomenon that may occur in the TSM control method.

Define the second order nonsingular terminal sliding hyperplane as Equation (27)

$$\boldsymbol{S} = \boldsymbol{z}_2 + \boldsymbol{\beta}^{-1}\dot{\boldsymbol{z}}_2^{p/q} \tag{27}$$

where $\boldsymbol{\beta} = \mathrm{diag}[\beta_1, \ldots, \beta_7]$ and $\beta_i > 0$ $(i = 1, \ldots, 7)$; p, q are the positive odds and satisfy $1 < p/q < 2$; $\dot{\boldsymbol{z}}_2^{p/q} = \left[\dot{z}_{21}^{p/q} \ldots \dot{z}_{27}^{p/q}\right]^{\mathrm{T}}$.

If the sliding hyperplane $\boldsymbol{S}$ arrives at $\boldsymbol{s} = 0$ within time t_r, then $\boldsymbol{z}_2$ and $\dot{\boldsymbol{z}}_2$ converge to zero in finite time and Equation (28) gives the convergence time

$$t_s = t_r + \boldsymbol{\beta}^{-q/p}\frac{p}{p-q}\left|\boldsymbol{z}_2\right|^{(p-q)/p} \tag{28}$$

By selecting suit parameters p, q and $\boldsymbol{\beta}$, then the rate of regulation $\boldsymbol{z}_2$ could be changed.

So the second order singular control law could be described from Equation (29) to Equation (32)

$$\boldsymbol{u} = \boldsymbol{u}_{eq} + \boldsymbol{u}_n \tag{29}$$

$$\boldsymbol{u}_{eq} = -\boldsymbol{B}^{-}\left(\boldsymbol{f} - \dot{\boldsymbol{x}}_{2d}\right) \tag{30}$$

$$\boldsymbol{u}_n = \int_0^t \boldsymbol{v}dt \tag{31}$$

$$\boldsymbol{v} = -\boldsymbol{B}^{-}\left(\boldsymbol{\beta}\frac{q}{p}\dot{\boldsymbol{z}}_2^{2-p/q} + \varepsilon\mathrm{sgn}(\boldsymbol{S})\right) \tag{32}$$

where $\boldsymbol{B}^{-} = \left(\boldsymbol{B}^{\mathrm{T}}\boldsymbol{B}\right)^{-1}\boldsymbol{B}^{\mathrm{T}}$.

Proof: Consider the Lyaponov function that is given as follows

$$V_2 = \frac{1}{2}\boldsymbol{S}^{\mathrm{T}}\boldsymbol{S} \tag{33}$$

The time derivative of V_2 can be obtained as Equation (34)

$$\begin{aligned} V_2 &= \boldsymbol{S}^{\mathrm{T}}\dot{\boldsymbol{S}} \\ &= \boldsymbol{S}^{\mathrm{T}}\left(\frac{p}{q}\boldsymbol{\beta}^{-1}\dot{\boldsymbol{z}}_2^{(p-q)/q}\left(\dot{\boldsymbol{f}} + \boldsymbol{B}\dot{\boldsymbol{u}} - \ddot{\boldsymbol{x}}_{2d} + \frac{q}{p}\boldsymbol{\beta}\dot{\boldsymbol{z}}_2^{2-p/q}\right)\right) \\ &= \boldsymbol{S}^{\mathrm{T}}\left(\frac{p}{q}\boldsymbol{\beta}^{-1}\dot{\boldsymbol{z}}_2^{(p-q)/q}(-\varepsilon\mathrm{sgn}(\boldsymbol{S}))\right) \\ &\leq -\varepsilon\frac{p}{q}\lambda_{\min}\left(\boldsymbol{\beta}^{-1}\dot{\boldsymbol{z}}_2^{(p-q)/q}\right)\|\boldsymbol{S}\| \\ &\leq 0 \end{aligned} \tag{34}$$

where $\lambda_{\min}(\bullet)$ stands for the smallest eigenvalue of vector $\bullet$.

So based on the Lyapunov stability theory, the subsystem (25) could track the virtual control x_{2d} exactly. As soon as the tracking error $\boldsymbol{z}_2 = 0$, the closed-loop system could achieve the accurate tracking for the $\boldsymbol{x}_{1d}$ under the action of $\boldsymbol{x}_{2d}$.

4. **Simulation Result.** The typical six orbital elements that establish the target satellite's orbit are $a = 6900000$m, $e = 0.001$, $i = 100°$, $\Omega = 70°$, $w = 30°$, $f = 125°$. The simulation parameters are given as Table 1.

TABLE 1. Simulation parameters

Description	Value
initial relative position	$\boldsymbol{\rho}_0 = [\ 0.5 \quad -10 \quad 0.2\ ]^{\mathrm{T}}$m
initial relative velocity	$\dot{\boldsymbol{\rho}}_0 = [\ -0.1 \quad 0.5 \quad 0.1\ ]^{\mathrm{T}}$m/s
desired relative position	$\boldsymbol{\rho}_d = [\ 0 \quad -2 \quad 0\ ]^{\mathrm{T}}$m
desired relative velocity	$\dot{\boldsymbol{\rho}}_d = [\ 0 \quad 0 \quad 0\ ]^{\mathrm{T}}$m/s
mass of chaser satellite	45kg
mass of target satellite	6kg
moment of inertia matrix of chaser	$\boldsymbol{I}_c = \mathrm{diag}(\ 8.0 \quad 6.0 \quad 11.5\ )^{\mathrm{T}}$kg·m^2
moment of inertia matrix of target	$\boldsymbol{I}_t = \mathrm{diag}(\ 0.9 \quad 1.5 \quad 0.8\ )^{\mathrm{T}}$kg·m^2
initial attitude quaternion of chaser	$\boldsymbol{q}_c = [\ 0.8 \quad -0.5 \quad 0.3162 \quad 0.1\ ]^{\mathrm{T}}$
initial attitude quaternion of target	$\boldsymbol{q}_t = [\ 1 \quad 0 \quad 0 \quad 0\ ]^{\mathrm{T}}$
initial attitude angular velocity of chaser	$\boldsymbol{\omega}_c = [\ 0 \quad 0 \quad 0\ ]^{\mathrm{T}}$rad/s
initial attitude angular velocity of target	$\boldsymbol{\omega}_t = [\ 0 \quad 0.05 \quad 0\ ]^{\mathrm{T}}$rad/s

The controller parameters are $c_i = 1$ $(i = 1, \ldots, 7)$, $\beta_i = 0.05$ $(i = 1, \ldots, 7)$, $p_i = 5$, $q = 3$, $\eta_i = 0.1$ $(i = 1, 2, 3)$, $\eta_i = 1$ $(i = 4, \ldots, 7)$. The disturbance force estimation $\hat{\boldsymbol{f}}_d$ and disturbance torque $\hat{\boldsymbol{M}}_d$ estimation are considered to be Gaussian distribution, and their standard deviation are $\frac{\hat{\boldsymbol{f}}_d}{10}$ and $\frac{\hat{\boldsymbol{M}}_d}{10}$ respectively. The disturbance force and disturbance torque are given as follows:

$$\boldsymbol{f}_d = [\ -1.5 \quad 2.5 \quad 1.0\ ]^{\mathrm{T}}\sin(0.03t) \times 10^{-5}\mathrm{m/s}^2$$

$$\boldsymbol{M}_d = [\ 3.0 \quad 2.0 \quad -2.5\ ]^{\mathrm{T}}\sin(0.05t) \times 10^{-4}\mathrm{N}\cdot\mathrm{m}$$

Figure 2 and Figure 3 show the relative position versus time and relative velocity versus time respectively. As can be seen in Figure 2, the relative position tracking is achieved in 40s, which implies that the chaser is driven to the desired position $\boldsymbol{\rho}_d = [\ 0 \quad -2 \quad 0\ ]^{\mathrm{T}}$m, and Figure 3 shows the relative velocity goes to zero so that there is no relative translational motion. The results in Figure 2 and Figure 3 demonstrate a good relative position tracking performance. Figure 4 shows the error quaternion versus time. As can be seen in

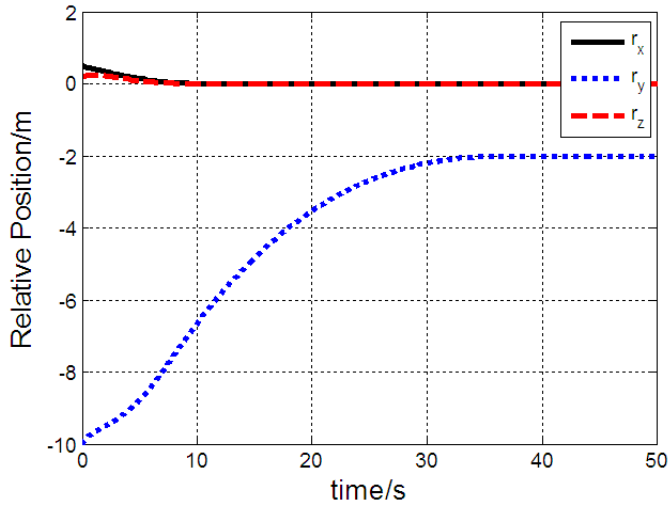

FIGURE 2. Relative position versus time

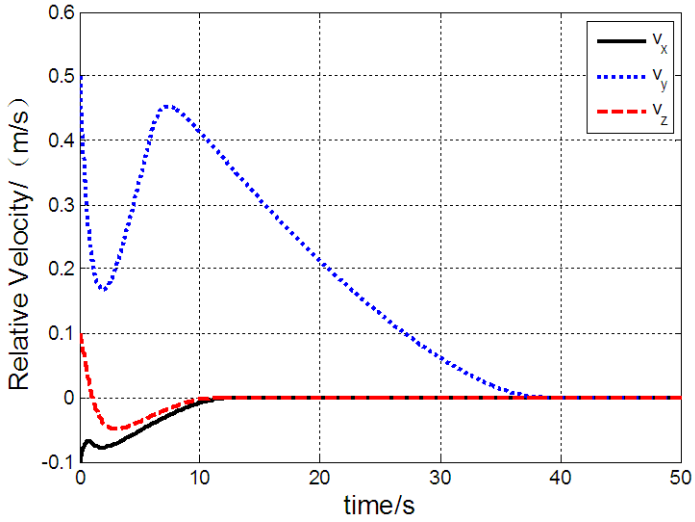

FIGURE 3. Relative velocity versus time

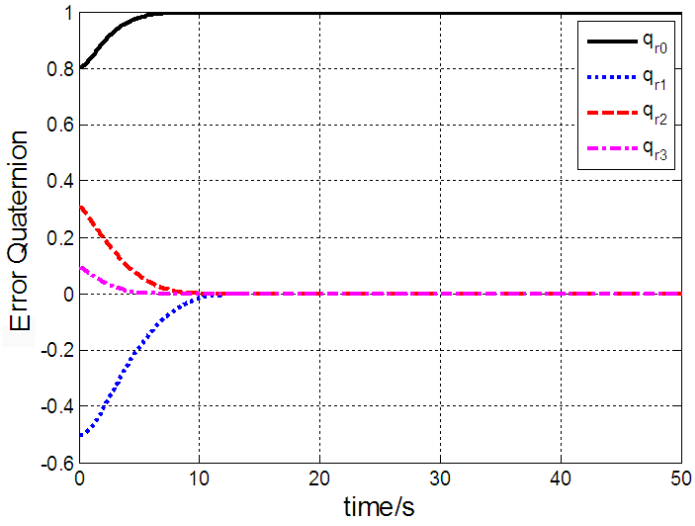

FIGURE 4. Error quaternion versus time

Figure 4, attitude synchronization is achieved in 15 seconds, which indicates the chaser's attitude is synchronized with the target's attitude. The results in Figure 2 demonstrate a good attitude synchronization performance. Overall, the simulation results in Figures 2-4 demonstrate that the stability of the six degrees-of-freedom closed-loop system can be guaranteed, and the proposed controller in this paper can achieve the relative position tracking and attitude synchronization precisely in the presence of external disturbances.

Figure 5 and Figure 6 show the control input applied to the chaser through control force and control torque, which indicates that the control force and torque are large for driving the chaser to the desired position and attitude quickly, but they decrease rapidly after the desired position and attitude are reached. Moreover, compared with the traditional SM and TSM control method, the proposed control law in this paper can resolve the chattering phenomenon very well, which can be demonstrated in Figure 5 and Figure 6. Actually, there is discontinuous part in the proposed controller because of the presence of the sign function. However, its integral, which is the actual control, is continuous and hence chattering is eliminated.

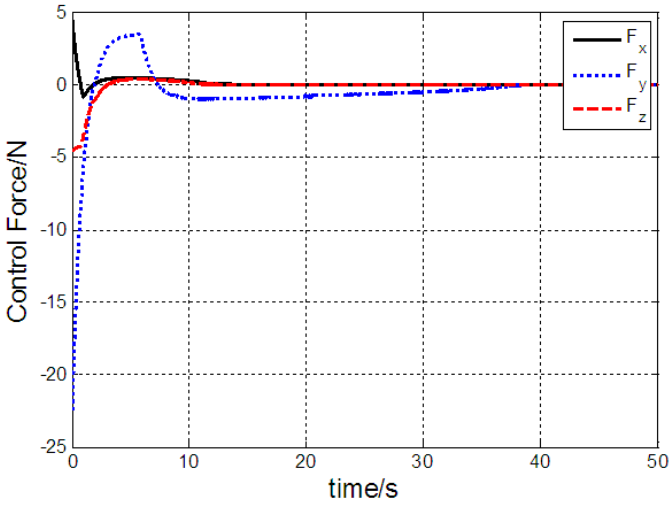

FIGURE 5. Control force versus time

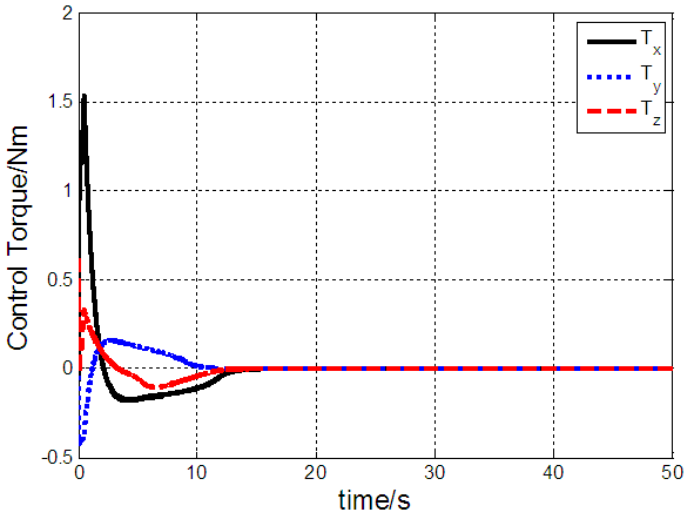

FIGURE 6. Control torque versus time

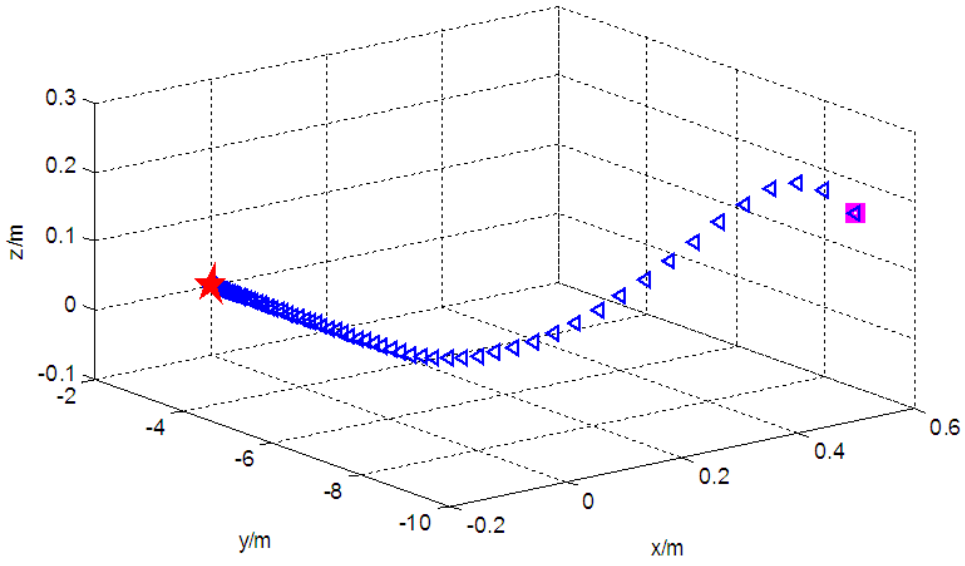

FIGURE 7. Relative position in the orbit coordinate system

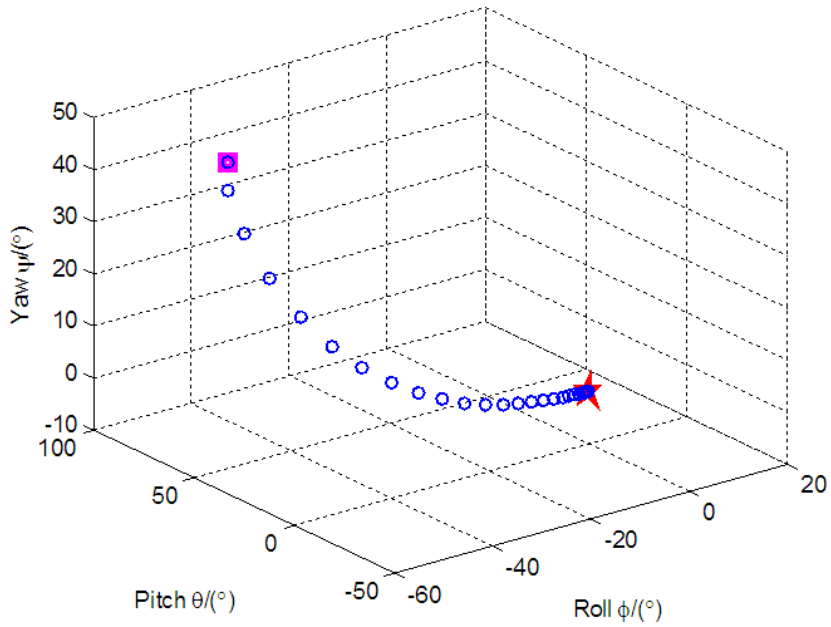

FIGURE 8. Euler angle of the relative attitude

Finally, the relative position in the orbit coordinate system and the relative Euler angle are shown in Figure 7 and Figure 8, which show the motion trajectory of the relative position and relative attitude respectively. Here, we transform attitude quaternion into Euler angle form. The spacecraft relative position and relative attitude trajectories can be seen in Figure 7 and Figure 8 more clearly. The simulation results in Figure 7 and Figure 8 also show that the proposed controller in this paper can achieve the relative position tracking and attitude synchronization precisely in the presence of external disturbances.

5. **Conclusions.** In this paper, the relative orbit and attitude integrated model for approaching a tumbling non-cooperative spacecraft is established. Then, considering the system uncertainty and disturbance, this paper proposes a controller design method by

combining the second order nonsingular terminal sliding mode control with the backstepping method. Based on the Lyapunov stability theory, the system stability has been proved. Numerical simulations demonstrate the efficiency of the controller that is proposed.

Acknowledgment. This work is partially supported by National Natural Science Foundation of China (Project No. 61203191) and Aeronautical Science Foundation of China (20140177006). The authors also gratefully acknowledge the helpful comments and suggestions of the reviewers, which have improved the presentation.

REFERENCES

[1] Y. Tsuda and S. Nakasuka, New attitude motion following control algorithm for capturing tumbling object in space, *Acta Astronautica*, vol.53, no.11, pp.847-861, 2003.

[2] A. Dutta and P. Tsiotras, Egalitarian peer-to-peer satellite refueling strategy, *Journal of Spacecraft and Rockets*, vol.45, no.3, pp.608-618, 2008.

[3] S. Matsumoto, Y. Ohkami and Y. Wakabayashi, Satellite capturing strategy using agile orbital servicing vehicle, Hyper-OSV, *Proc. of 2002 IEEE International Conf. on Robotics and Automation*, Washington, DC, pp.2309-2314, 2002.

[4] I. Kawano, M. Mokuno and T. Kasai, Result of autonomous rendezvous docking experiment of engineering test satellite-VII, *Journal of Spacecraft and Rockets*, vol.38, no.1, pp.105-111, 2001.

[5] D. A. Whelan, E. A. Adler and S. B. Wilson, Darpa orbital express program: Effecting a revolution in space-based systems, *Proc. of SPIE*, San Diego, USA, pp.48-56, 2000.

[6] A. B. Bosse, W. J. Barnds, M. A. Brown et al., SUMO: Spacecraft for the universal modification of orbits, *Proc. of SPIE*, Orlando, FL, the United States, pp.36-46, 2004.

[7] S. C. Lo and Y. P. Chen, Smooth sliding-mode control for spacecraft attitude tracking maneuvers, *Journal of Guidance, Control, and Dynamics*, vol.18, no.6, pp.1345-1349, 1995.

[8] F. Terui, Position and attitude control of a spacecraft by sliding mode control, *Proc. of American Control Conference*, Philadelphia, PA, the United States, pp.217-221, 1998.

[9] K. S. Kim and Y. Kim, Robust backstepping control for slew maneuver using nonlinear tracking function, *IEEE Trans. Control Systems Technology*, vol.11, no.6, pp.822-829, 2003.

[10] M. Krstić and P. Tsiotras, Inverse optimal stabilization of a rigid spacecraft, *IEEE Trans. Automatic Control*, vol.44, no.5, pp.1042-1049, 1999.

[11] S. T. Venkataraman and S. Gulati, Control of nonlinear systems using terminal sliding modes, *Journal of Dynamic Systems, Measurement, and Control*, vol.115, no.3, pp.554-560, 1993.

[12] Z. H. Man, A. P. Paplinski and H. R. Wu, A robust MIMO terminal sliding mode control scheme for rigid robotic manipulators, *IEEE Trans. Automatic Control*, vol.39, no.12, pp.2464-2469, 1994.

[13] Y. Feng, X. Yu and Z. Man, Non-singular terminal sliding mode control of rigid manipulators, *Automatica*, vol.38, no.12, pp.2159-2167, 2002.

[14] M. Sanjoy and M. Chitralekha, Adaptive second order terminal sliding mode controller for robotic manipulators, *Journal of the Franklin Institute*, vol.351, no.4, pp.2356-2377, 2014.

[15] Y. Feng, F. L. Han and X. H. Yu, Chattering free full-order sliding-mode control, *Automatic*, vol.50, no.4, pp.1310-1314, 2014.

[16] H. R. Li, Z. B. Jiang and N. Kang, Sliding mode disturbance observer-based fractional second-order nonsingular terminal sliding mode control for PMSM position regulation system, *Mathematical Problems in Engineering*, vol.2015, 2015.

[17] W. Lu, Y. H. Geng and X. Q. Chen, Coupled control of relative position and attitude for on-orbit servicing spacecraft with respect to target, *Acta Aeronautica et Astronautica Sinica*, vol.32, no.5, pp.857-865, 2011.

[18] D. Gao, J. Luo and W. Ma, Nonlinear optimal control of spacecraft approaching and tracking a non-cooperative maneuvering object, *Journal of Astronautics*, vol.34, no.6, pp.773-781, 2013.

[19] X. Ming and H. Pan, Nonlinear optimal control of spacecraft approaching a tumbling target, *Aerospace Science and Technology*, vol.15, no.2, pp.79-89, 2011.

[20] L. Sun and W. Huo, Robust adaptive relative position tracking and attitude synchronization for spacecraft rendezvous, *Aerospace Science and Technology*, vol.41, pp.28-35, 2015.

[21] Q. Z. Zhang, Y. Q. Jin and Z. Y. Kang, Coupled control of relative position and attitude for servicing spacecraft approaching the target in close proximity, *System Engineering and Electronics*, vol.37, no.1, pp.141-147, 2015.

[22] J. R. Li, H. Y. Li and G. J. Tang, Adaptive sliding mode control for approach to uncontrolled rotating satellite, *Journal of Astronautics*, vol.32, no.4, pp.815-822, 2011.

[23] J. Yang, S. H. Li, and J. Y. Su, Continuous nonsingular terminal sliding mode control for systems with mismatched disturbances, *Automatic*, vol.49, no.7, pp.2287-2291, 2013.

[24] Q. X. Lan, J. Yang and S. H. Li, Finite-time control for 6DOF spacecraft formation flying systems, *Journal of Aerospace Engineering*, vol.28, no.5, pp.1-19, 2015.

[25] H. L. Liu, X. P. Shi and L. Li, Nonsingular terminal sliding mode control for approach to non-cooperative satellite, *The 25th Chinese Control and Decision Conference*, Qingdao, China, 1524-1529, 2015.